Rayleigh-Taylor linear growth at an interface between an elastoplastic solid and a viscous liquid

A. R. Piriz*
E.T.S.I. Industriales, Instituto de Investigaciones Energéticas and CYTEMA, Universidad de Castilla–La Mancha, 13071 Ciudad Real, Spain

Y. B. Sun
Institute of Modern Physics, Chinese Academy of Science, 730000 Lanzhou, People's Republic of China

N. A. Tahir
GSI Helmholtzzentrum für Schwerionenforschung Darmstadt, Planckstrasse 1, 64291 Darmstadt, Germany
(Received 24 January 2014; revised manuscript received 11 April 2014; published 30 June 2014)

A previously developed model for the Rayleigh-Taylor instability at an interface between an elastoplastic solid and a viscous fluid [Piriz, Sun, and Tahir, Phys. Rev. E **88**, 023026 (2013)] has been used for calculating the time evolution of the perturbations in terms of the mechanical properties of the solid and the liquid, as well as of the initial amplitude ξ_0 and the wavelength λ of the perturbation. Four kinds of possible evolution are found: two stable and two unstable, depending on their positions in the space of parameters (ξ_0,λ). All of them present some features that are independent of the solid properties and that are determined only by the liquid viscosity.

DOI: 10.1103/PhysRevE.89.063022 PACS number(s): 47.20.−k, 52.58.Hm, 52.50.Lp

I. INTRODUCTION

The Rayleigh-Taylor instability (RTI) in accelerated solids was first considered by Miles in 1966 by means of an approximate theoretical analysis [1]. Since then, numerous theoretical, numerical, and experimental investigations have been performed [2–15]. The interest in this problem has grown in the last decade mainly because of its application as a tool for determining mechanical properties of solids at the high strains and high strain rates that can be achieved in experiments driven by intense laser pulses [16–22]. These experiments have allowed for extending the pioneering work by Barnes *et al.* performed with high explosives [3,4]. In addition, the RTI in solids is of relevance in geophysics as it plays a role in the thickening of the lithosphere beneath mountain belts [23–26], as well as in astrophysics as it seems to be present in starquakes occurring in slowly accreting neutron stars [27].

On the other hand, the RTI in solids is also of relevance for the design of some experiments on high-energy-density matter (HEDM) such as the Laboratory Planetary Sciences (LAPLAS) experiment planned in the framework of the Facility for Antiproton and Ion Research (FAIR) presently under construction at Darmstadt (Germany) [28–36]. LAPLAS consists of the implosion of a thick W or Ta cylindrical shell driven by an intense heavy-ion beam with a ring-shaped focal spot. The tamped expansion of the annular region (the absorber) heated by the ion beam drives the implosion of the internal layers (the pusher) leading to the low-entropy compression of a sample material that is placed in the axial region. In the course of the heating process the absorber region is melted while the pusher remains in the solid state. Thus during the acceleration phase it can be considered that the absorber is a viscous liquid and that the pusher is a solid with elastoplastic material properties.

The LAPLAS conditions are expected to be similar to those present in magnetically imploded liners for which the external layers can be melted depending on the intensity and time history of the driving electrical current [37,38]. In both cases, a solid-liquid imploding interface is generated that is susceptible to being affected by the onset of the Rayleigh-Taylor instability [3,4,16–22,39–47].

At this type of interface the RTI has previously been considered only for the case in which the solid is perfectly elastic [42,43]. Additionally, we have recently studied the RTI at an elastoplastic-solid–viscous-liquid interface, but we restricted ourselves to the problem of finding the stability region as it is determined by the initial amplitude ξ_0 and the wavelength λ of the perturbations, as well as by the mechanical properties of the solid and the liquid given by the respective rheological models [48]. However, the complete solution of the problem providing the different stable and unstable evolutions of the perturbation amplitude is necessary for the better understanding and design of experiments on HEDM, as well as for its application to the analysis of experiments for determining the mechanical properties of solids under extreme conditions. In particular, the case under consideration in this work involving the presence of a viscous liquid may indicate a way for using the RTI also for the experimental determination of the viscosity of melted metals at megabar pressures and temperatures of a few thousand kelvin. The viscosity of liquid metals under such conditions is considered as one of the most important and least known parameters in geophysics and planetary sciences [49–53].

In this work we use the model of Ref. [48] for obtaining explicit analytical solutions that describe the linear evolution of the perturbation amplitude in the different stable and unstable regimes. Such regimes are determined by the stability boundary which depends on the initial amplitude and wavelength of the perturbation, and on the material properties of the solid and the liquid. The model is expected to be

*roberto.piriz@uclm.es

useful in conceiving a new experiment for the measurement of the viscosity of liquid metals under high-energy-density conditions. In addition, although it deals with the RTI in planar geometry it can be used to understand some aspects of the LAPLAS experiment related to the instability in the presence of a liquid metal pushing an elastoplastic solid.

II. FORMULATION OF THE PROBLEM AND the PHYSICAL MODEL

The physical situation is the same as described in Ref. [48], in which we have an incompressible solid plate of density ρ_2 thick enough so that it can be considered to occupy the complete half space $y < 0$. This assumption requires that the plate thickness h is such that $kh \gg 1$, where $k = 2\pi/\lambda$ is the perturbation wave number. In the same manner, the half space $y > 0$ is filled with an incompressible liquid of density $\rho_1 < \rho_2$.

For the constitutive properties of the liquid we assume that it is a Newtonian fluid characterized by a dynamical viscosity μ [42–44]. For the solid we assume that it can be described by a nonlinear Pandlt-Reuss model with von Mises stress criterion that is characterized by a constant shear modulus G and a constant yield strength Y [46,47,53,54]. This model provides a suitable expression for the deviatoric part of the stress tensor S_{ij} that has been derived in Ref. [47] by considering an irrotational perturbed velocity field [$v_x = \dot{\xi}(t)e^{ky}\cos kx$, and $v_y = \dot{\xi}(t)e^{ky}\sin kx$]. In particular, the normal component S_{yy} is given by

$$S_{yy} = \begin{cases} 2kG\xi e^{ky}\sin kx & \text{if} \quad \xi \leqslant \xi_p, \\ \frac{1}{\sqrt{3}}Y\sin kx & \text{if} \quad \xi \geqslant \xi_p. \end{cases} \tag{1}$$

As discussed in Refs. [46–48], we also consider that the solid has been pushed and accelerated by the fluid for a very long time until the time $t = 0$, with a constant and uniform pressure p_0 applied on the interface ($y = 0$) so that, at $t \geqslant 0$, the interface has an acceleration $\vec{a} = -g\mathbf{e}_y$ ($g = p_0/\rho h$). Then, at $t = 0$, a ripple $\delta p = p_0(\xi_0/h)e^{-k|y|}\sin kx$ is superposed on the uniform pressure p_0. Although this approach is entirely equivalent to the more usual one considering a uniform pressure at $t = 0$ and an initial corrugation ξ_0 on the interface, it allows for a more realistic description of the situation expected in the LAPLAS experiment. In fact, a nonuniform pressure will be generated at the interface by the irradiation nonuniformities produced in creating an effective annular focal spot by a rf wobbler system that will rotate the ion beam [55–57].

On the other hand, Eq. (1) shows that the onset of the plastic flow occurs first at $y = 0$ where the maximum deformation takes place. Then, as the perturbation grows, the yielded region progresses toward the solid interior ($y \leqslant 0$). By keeping in mind that we are dealing with the average motion of the region affected by the instability and that it expands over a region with thickness of the order of k^{-1}, we can expect that the onset of plastic flow will not affect the RTI until this entire solid region has yielded [47]. Therefore, Eq. (1) is evaluated at $y \approx -k^{-1}$ and hereafter we will take $e^{ky} \approx 1/3$.

With the previous assumptions the time evolution of the perturbation amplitude $\xi(t)$ has been found to be described by the following differential equation [48]:

$$\ddot{\xi} + \frac{2\mu k^2}{\rho_2+\rho_1}\dot{\xi} - A_T kg(\xi+\xi_0) = -\begin{cases} \frac{2k^2G}{\rho_2+\rho_1}\xi & \text{for} \quad \xi \leqslant \xi_p, \\ \frac{\sqrt{3}Yk}{\rho_2+\rho_1} & \text{for} \quad \xi \geqslant \xi_p, \end{cases} \tag{2}$$

where $A_T = (\rho_2 - \rho_1)/(\rho_2 + \rho_1)$ is the Atwood number, $\xi_p = \sqrt{3}Y/(2kG)$ is the perturbation amplitude when the transition from the elastic to the plastic regime takes place (the EP transition), and the overdots indicate time derivatives. The reader is referred to Ref. [48] for more details about the derivation of Eq. (2) (see also Refs. [41,43–47]). The initial conditions for the previous equation are $\xi(0) = \dot{\xi}(0) = 0$.

It is convenient to rewrite Eq. (2) by introducing the following dimensionless variables:

$$z = \frac{\xi}{\xi_0}, \quad \tau = t\sqrt{A_T kg}. \tag{3}$$

Thus Eq. (2) reads

$$\ddot{z} + 2D\dot{z} = \begin{cases} 1 - \Lambda z & \text{for} \quad z \leqslant z_p, \\ z - X & \text{for} \quad z \geqslant z_p, \end{cases} \tag{4}$$

where we have used the following definitions:

$$\Lambda = \hat{\lambda}^{-1} - 1, \quad X = \hat{\xi}^{-1} - 1, \quad D = \frac{D_0}{\hat{\lambda}^{3/2}}, \tag{5}$$

and

$$\hat{\lambda} = \frac{(\rho_2-\rho_1)g\lambda}{4\pi G}, \quad \hat{\xi} = \frac{(\rho_2-\rho_1)g\xi_0}{\sqrt{3}Y}, \qquad D_0 = \frac{\mu g}{2\sqrt{2}}\sqrt{\frac{A_T(\rho_2-\rho_1)}{G^3}}. \tag{6}$$

In addition, we have

$$1 - \Lambda z_p = z_p - X, \quad z_p = \frac{\hat{\lambda}}{\hat{\xi}}, \tag{7}$$

and the corresponding initial conditions read

$$z(0) = \dot{z}(0) = 0. \tag{8}$$

In order to solve Eq. (4) we introduce the following transformations:

$$x_1 = (1 - \Lambda z)e^{D\tau} \quad \text{for} \quad z \leqslant z_p, \tag{9}$$

$$x_2 = (z - X)e^{D\tau} \quad \text{for} \quad z \geqslant z_p. \tag{10}$$

Thus, the two branches of Eq.(4) transform as follows:

$$\ddot{x}_1 = (D^2 - \Lambda)x_1 \quad \text{for} \quad z \leqslant z_p, \tag{11}$$

$$\ddot{x}_2 = (1 + D^2)x_2 \quad \text{for} \quad z \geqslant z_p, \tag{12}$$

and these equations must satisfy the following conditions:

$$x_1(0) = 1, \quad \dot{x}_1(0) = D, \tag{13}$$

$$x_1(\tau_p) = x_2(\tau_p) = x_p, \tag{14}$$

$$\dot{x}_1(\tau_p) = \dot{x}_{1p}, \quad \dot{x}_2(\tau_p) = \dot{x}_{2p}, \tag{15}$$

where τ_p is the time when the EP transition takes place.

A. Stability and EP transition boundaries

The boundaries for the stability and for the EP transition were obtained in Ref. [48] and here we will briefly review the main results in order to reference them in the following paragraphs with a consistent notation.

For determining the stability boundary we have to take into account that if the interface is stable the amplitude $z(\tau)$ must have a maximum at a certain time $\tau = \tau_m$. Therefore, we must have $\dot{z}(\tau_m) = 0$ and $\ddot{z}(\tau_m) \leqslant 0$. If instead $\ddot{z}(\tau_m) \geqslant 0$ the extreme will be an inflection point and the interface will be unstable. Therefore, the condition for marginal stability that determine the instability threshold reads [46,47]

$$\dot{z}\left(\tau_m^{\rm th}\right) = \ddot{z}\left(\tau_m^{\rm th}\right) = 0, \tag{16}$$

where the index "th" indicates that we are considering solutions that are marginally stable so that they are lying on the instability threshold, and $\tau_m^{\rm th}$ is the instant when such solutions achieve the maximum perturbation amplitude.

As we can see from Eq. (4), the conditions for marginal stability are never satisfied for $\lambda > 1$ ($z \geqslant 0$), and therefore the interface will be unstable for any value of the dimensionless amplitude $\hat{\xi}$, as happens for purely elastic solids [29,42,47]. This is because, for $\lambda > 1$, the buoyancy force $(\rho_2 - \rho_1)g\xi$ always overcomes the mechanical force S_{yy} for any value of ξ.

We start with the branch for $z \leqslant z_p$, and upon integration of Eq. (11) we get

$$\dot{x}_1 = -\sqrt{(D^2 - \Lambda)x_1^2 + \Lambda}, \tag{17}$$

where the negative sign is taken because for solutions lying on the stability threshold we must have $z \geqslant 0$, $\dot{z} = 0$, and $\ddot{z} \leqslant 0$. Therefore, from Eq. (4) for $z \leqslant z_p$ we see that $1 - \Lambda z \leqslant 0$ and, thus, $\dot{x}_1 \leqslant 0$.

Now, by integrating Eq. (17) from $\tau = 0$ to $\tau = \tau_p^{\rm th}$ ($\tau_p^{\rm th}$ is the instant when the marginally stable solution undergoes the transition to the plastic regime), and then taking into account Eq. (14), we obtain

$$\tau_p^{\rm th} = -\frac{1}{\sqrt{\Lambda - D^2}}\left[\sin^{-1}\left(\sqrt{\frac{\Lambda - D^2}{\Lambda}}\, x_p^{\rm th}\right) - \sin^{-1}\left(\sqrt{\frac{\Lambda - D^2}{\Lambda}}\right)\right]. \tag{18}$$

By proceeding in a similar manner with the branch for $z \geqslant z_p$, we perform a first integration of Eq. (12):

$$\dot{x}_2^2 = \left(\dot{x}_{2p}^{\rm th}\right)^2 + (1 + D^2)\left[x_2^2 - \left(x_p^{\rm th}\right)^2\right], \tag{19}$$

where we have taken into account Eqs. (13) and (14). Since the solutions lying on the instability boundary must satisfy Eqs. (16), it turns out from Eq. (4) (for $z \geqslant z_p$) and from the derivative of Eq. (12) that $x_2(\tau_m^{\rm th}) = \dot{x}_2(\tau_m^{\rm th}) = 0$. Then Eq. (19) yields

$$\dot{x}_{2p}^{\rm th} = -x_p^{\rm th}\sqrt{1 + D^2}. \tag{20}$$

By evaluating the derivative of Eq. (9) at $\tau = \tau_p^{\rm th}$ and using Eqs. (17) and (20), we get

$$x_p^{\rm th} = -\sqrt{\frac{\hat{\lambda}}{1 + 2D(D + \sqrt{1 + D^2})}}. \tag{21}$$

Since from Eq. (9) we have $x_p^{\rm th} = [1 - \Lambda(\hat{\xi}_{\rm th}/\hat{\lambda})]e^{D\tau_p^{\rm th}}$, then Eq. (21) yields the following equation for the instability threshold:

$$\hat{\xi}_{\rm th} = \frac{1 - \hat{\lambda}}{1 - x_p^{\rm th} e^{-D\tau_p^{\rm th}}}, \tag{22}$$

with $\tau_p^{\rm th}$ given by Eq. (18).

In a similar manner, we can find the boundary for the EP transition by taking into account that it occurs when the maximum amplitude z_m^e of the purely elastic oscillations (for $z \leqslant z_p$) becomes equal to z_p at the transition time τ_e: $z_m^e = z_p(\tau_e) = \hat{\xi}_{ep}/\hat{\lambda}$. Therefore, $z(\tau_e) = z_m^e$ and $\dot{z}(\tau_e) = 0$, and the derivative of Eq. (9) yields

$$\dot{x}_{1e} = \dot{x}_1(\tau_e) = x_{1e}D = [1 - \Lambda(\hat{\xi}_{ep}/\hat{\lambda})]e^{D\tau_e}, \tag{23}$$

and combining this equation with Eq. (17) evaluated at $\tau = \tau_e$ we find that $x_{1e} = -1$. On the other hand, the integral of Eq. (17) between $\tau = 0$ and $\tau = \tau_e$ gives the following expression for τ_e:

$$\tau_e = \frac{2}{\sqrt{\Lambda - D^2}} \sin^{-1}\left(\sqrt{\frac{\Lambda - D^2}{\Lambda}}\right). \tag{24}$$

Thus, from Eq. (23) the boundary for the EP transition is given by the following equation:

$$\hat{\xi}_{ep} = \frac{1 - \hat{\lambda}}{1 + e^{-D\tau_e}}. \tag{25}$$

Taking into account the definition of D by Eq. (5) and the expressions for $\tau_p^{\rm th}$ and τ_e given respectively by Eqs. (18) and (24), Eqs. (22) and (25) give respectively the instability threshold and the boundary for the EP transition as the functions $\hat{\xi}_{\rm th}(\hat{\lambda})$ and $\hat{\xi}_{ep}(\hat{\lambda})$ with D_0 as a parameter.

These two boundaries are represented in Fig. 1 for different values of D_0 (0, 0.05, 0.5, and 5). As noticed in Refs. [46–48], $\hat{\xi}_{ep} \leqslant \hat{\xi}_{\rm th}$ always, and the two boundaries become the same in the limit of high viscosity $D_0 \gg 1$, so that $\hat{\xi}_{ep}^{\infty} = \hat{\xi}_{\rm th}^{\infty} = 1 - \hat{\lambda}$.

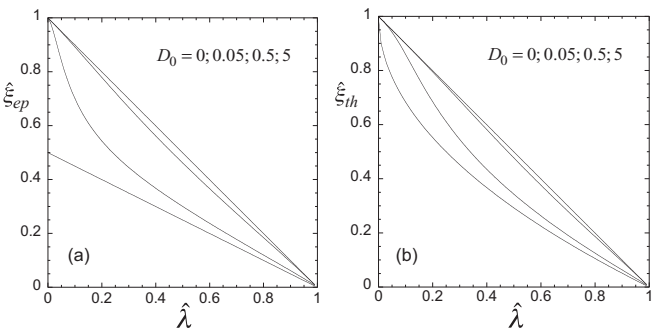

FIG. 1. (a) Boundary for the EP transition, and (b) stability region, for different values of the dimensionless viscosity D_0. D_0 increases in the curves from bottom to top.

B. Time evolution of the perturbation amplitude

We can obtain the linear growth of the RTI upon integration of Eq. (4). For this, we first integrate the transformed Eq. (11) for $z \leqslant z_p$ with the initial conditions given by Eq. (13). Then, we invert the transformation given by Eq. (9) to find $z(\tau)$ for this branch. We proceed in the same manner with Eq. (12) for the branch $z \geqslant z_p$, with the conditions given by Eqs. (14) and (15) to get $x_2(\tau)$, and then we invert the transformation of Eq. (10) to obtain $z(\tau)$ for the other branch.

The resulting time evolution $z(\tau)$ will depend on the parameters $\hat{\xi}$, $\hat{\lambda}$, and D_0 and, according to the position in the space $(\hat{\xi},\hat{\lambda})$ shown in Fig. 1 (see also Fig. 2), we can have two kinds of stable solution and two kinds of unstable solution.

1. Stable solutions

The two stable cases correspond to $\hat{\lambda} \leqslant 1$, for $\hat{\xi} \leqslant \hat{\xi}_{ep}$ and for $\hat{\xi}_{ep} \leqslant \hat{\xi} \leqslant \hat{\xi}_{\rm th}$, respectively:

$$z(\tau) = \begin{cases} \frac{1}{\Lambda}\left\{1 - e^{-D\tau}\left[\cos(\sqrt{\Lambda - D^2}\,\tau) + \frac{D}{\sqrt{\Lambda - D^2}}\sin(\sqrt{\Lambda - D^2}\,\tau)\right]\right\}, & \tau \leqslant \tau_p, \\ X + \frac{1}{2}e^{-D\tau}\left[\left(x_p + \frac{\dot{x}_{2p}}{\sqrt{1+D^2}}\right)e^{\sqrt{1+D^2}(\tau-\tau_p)} + \left(x_p - \frac{\dot{x}_{2p}}{\sqrt{1+D^2}}\right)e^{-\sqrt{1+D^2}(\tau-\tau_p)}\right], & \tau_p \leqslant \tau \leqslant \tau_m, \\ z_m - \frac{X - z_m}{\Lambda}\left[1 - e^{-D(\tau-\tau_m)}\left(\cos[\sqrt{\Lambda - D^2}(\tau-\tau_m)] + \frac{D}{\sqrt{\Lambda - D^2}}\sin[\sqrt{\Lambda - D^2}(\tau-\tau_m)]\right)\right], & \tau \geqslant \tau_m, \end{cases} \tag{26}$$

where $x_p = (1 - \Lambda z_p)e^{D\tau_p}$, and $\dot{x}_{2p}$ is obtained from Eqs. (9) and (10). For this last purpose, we take the derivatives of those equations, evaluate them at $\tau = \tau_p$, and eliminate $\dot{z}_p$ from the two resulting expressions [using also Eq. (17)]:

$$\dot{x}_{2p} = \frac{1}{\Lambda}\left[x_p D(1+\Lambda) + \sqrt{(D^2 - \Lambda)x_p^2 + \Lambda}\right]. \tag{27}$$

In addition, τ_p is given by an implicit equation obtained by evaluating the first branch of Eq. (26) at $\tau = \tau_p$ when $z = z_p = \hat{\lambda}/\hat{\xi}$:

$$\frac{\hat{\lambda}}{\hat{\xi}} = \frac{1}{\Lambda}\left\{1 - e^{-D\tau_p}\left[\cos(\sqrt{\Lambda - D^2}\,\tau_p) + \frac{D}{\sqrt{\Lambda - D^2}}\sin(\sqrt{\Lambda - D^2}\,\tau_p)\right]\right\}. \tag{28}$$

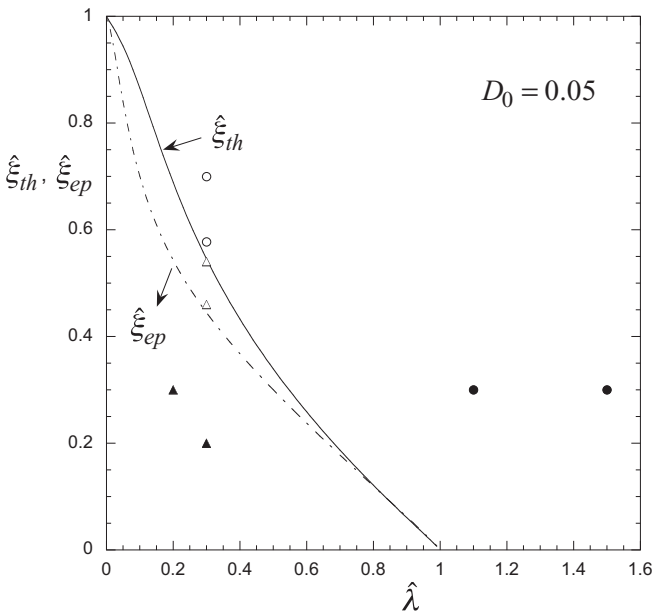

FIG. 2. Stability region for the dimensionless viscosity $D_0 = 0.05$. The boundary for the EP transition is indicated by the dotted line. Dots correspond to typical cases represented in Figs. 3–5.

On the other hand, in Eq. (26) τ_m is the time at which the plastic branch of Eq. (26) $(\tau_p \leqslant \tau \leqslant \tau_m)$ achieves the maximum amplitude $z_m = z(\tau_m)$ and then for $\tau \geqslant \tau_m$, the evolution of the amplitude goes back to the purely elastic regime in which, provided that $D^2 < \Lambda$, it remains oscillating around a maximum with damped oscillations [curves (a) and (b) in Fig. 3]:

$$\tau_m = \tau_p + \frac{1}{2\sqrt{1+D^2}} \times \ln\left\{\frac{(x_p\sqrt{1+D^2} - \dot{x}_{2p})(\sqrt{1+D^2} + D)}{(x_p\sqrt{1+D^2} + \dot{x}_{2p})(\sqrt{1+D^2} - D)}\right\}. \tag{29}$$

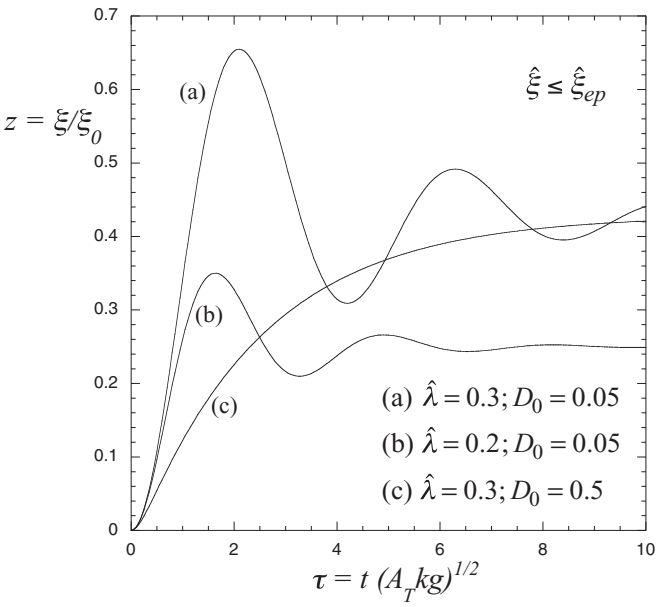

FIG. 3. Stable solutions in the purely elastic regime ($\hat{\lambda} \leqslant 1$ and $\hat{\xi} \leqslant \hat{\xi}_{ep}$). Curves (a) and (b) correspond to oscillatory damped solutions ($D^2 < \Lambda$), and curve (c) corresponds to an overdamped solution ($D^2 > \Lambda$).

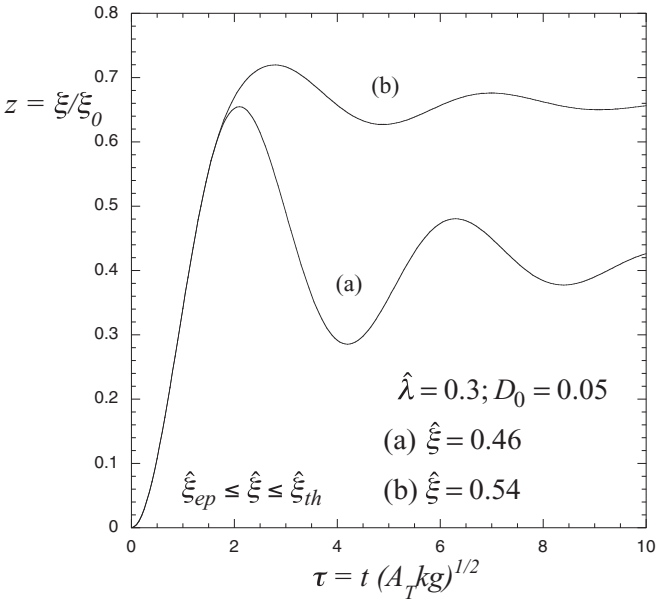

FIG. 4. Stable solutions in the plastic regime ($\hat{\lambda} \leqslant 1$ and $\hat{\xi}_{ep} \leqslant \hat{\xi} \leqslant \hat{\xi}_{\rm th}$).

Instead, if $D^2 > \Lambda$, then the amplitude goes to its maximum asymptotically in an overdamped growth [curve (c) in Fig. 3]. In this case, the amplitude grows up to a maximum $z_{\max} = \hat{\lambda}/(1-\hat{\lambda})$ which is always less than z_p, so that the overdamped stable growth remains always in the purely elastic region.

The triangles in Fig. 2 (full and empty) indicate the typical loci of the two kinds of stable solution in the space $(\hat{\xi},\hat{\lambda})$. In Fig. 3 we show typical stable solutions in the purely elastic region ($\hat{\xi} \leqslant \hat{\xi}_{ep}$) corresponding to the full triangles in Fig. 2. In this region the time evolution of the perturbation amplitude is independent of $\hat{\xi}$ and the amplitude of the oscillations for $\tau > \tau_m$ increases with $\hat{\lambda}$ up to infinity for $\hat{\lambda} = 1$. Curves (a) and (b) represent two typical cases for $\hat{\lambda} = 0.3$ and 0.2, respectively, and for $D_0 = 0.05$. In this region we may also have overdamped solutions when $D^2 > \Lambda$ [curve (c) for $\hat{\lambda} = 0.3$ and $D_0 = 0.5$].

In Fig. 4 we show two typical examples of the other kind of stable solution corresponding to the plastic region ($\hat{\xi}_{ep} \leqslant \hat{\xi} \leqslant \hat{\xi}_{\rm th}$) for $\hat{\lambda} = 0.3$ and $D_0 = 0.05$. Curve (a) corresponds to a case close to the EP transition, and curve (b) to one that is close to the instability threshold. As we can see the maximum amplitude of the perturbation increases as we approach the instability threshold but the amplitude of the elastic oscillations occurring for $\tau \geqslant \tau_m$ decreases. The general behavior of the stable solutions is qualitatively similar to that found for an elastoplastic-solid–inviscid-fluid interface [46,47], except for the viscous damping as $e^{-D\tau}$ of the elastic oscillations after τ_m.

2. *Unstable solutions*

As in the case of Refs. [46,47] involving an inviscid fluid, we have two kinds of unstable solution for values of $(\hat{\xi},\hat{\lambda})$ lying beyond the stability boundary as in the cases indicated in Fig. 2 with full and empty circles. One case corresponds to $\hat{\lambda} \leqslant 1$ and $\hat{\xi} \geqslant \hat{\xi}_{\rm th}$, like the two examples indicated in Fig. 2 with empty circles. This kind of unstable solution is described by the following equation ($\hat{\lambda} \leqslant 1$):

$$z(\tau) = \begin{cases} \frac{1}{\Lambda}\left\{1 - e^{-D\tau}\left[\cos(\sqrt{\Lambda - D^2}\,\tau) + \frac{D}{\sqrt{\Lambda - D^2}}\sin(\sqrt{\Lambda - D^2}\,\tau)\right]\right\}, & \tau \leqslant \tau_p, \\ X + \frac{1}{2}e^{-D\tau}\left[\left(x_p + \frac{\dot{x}_{2p}}{\sqrt{1+D^2}}\right)e^{\sqrt{1+D^2}(\tau-\tau_p)} + \left(x_p - \frac{\dot{x}_{2p}}{\sqrt{1+D^2}}\right)e^{-\sqrt{1+D^2}(\tau-\tau_p)}\right], & \tau \geqslant \tau_p. \end{cases} \tag{30}$$

In a similar manner, the other kind of unstable solution occurring for $\hat{\lambda} \geqslant 1$ ($\Lambda \leqslant 1$) is given by the following expression:

$$z(\tau) = \begin{cases} \frac{1}{\Lambda}\left\{1 - e^{-D\tau}\left[\cosh(\sqrt{D^2 - \Lambda}\,\tau) + \frac{D}{\sqrt{\Lambda - D^2}}\sinh(\sqrt{D^2 - \Lambda}\,\tau)\right]\right\}, & \tau \leqslant \tau_p, \\ X + \frac{1}{2}e^{-D\tau}\left[\left(x_p + \frac{\dot{x}_{2p}}{\sqrt{1+D^2}}\right)e^{\sqrt{1+D^2}(\tau-\tau_p)} + \left(x_p - \frac{\dot{x}_{2p}}{\sqrt{1+D^2}}\right)e^{-\sqrt{1+D^2}(\tau-\tau_p)}\right], & \tau \geqslant \tau_p. \end{cases} \tag{31}$$

In Fig. 5 we show two typical examples for $\hat{\lambda} = 0.3$, corresponding to the empty circles in Fig. 2. One is for $\hat{\xi} = 0.58$, which is above but close to the instability threshold [curve (a)], and the other one for the case with $\hat{\xi} = 0.78$ [curve (b)] relatively far from the threshold. We can see that after an initial common elastic phase of growth, the growth rate becomes larger in the latter case. However, the asymptotic growth rate σ_∞ (for $\tau \to \infty$) turns out to be the same. In fact, from Eq. (30), we get

$$\frac{\xi_\infty}{\xi_0} = \frac{1}{2}\left(x_p + \frac{\dot{x}_{2p}}{\sqrt{1+D^2}}\right)e^{-\sqrt{1+D^2}\tau_p}\,e^{\sigma_\infty \tau}, \tag{32}$$

where

$$\sigma_\infty = \sqrt{1+D^2} - D. \tag{33}$$

This growth rate is the same as the one corresponding to the evolution of the RTI in a pure viscous fluid. That is, the asymptotic growth rate does not contains any information regarding the mechanical properties of the solid. This information, however, remains in the effective initial amplitude $= \frac{\xi_0}{2}(x_p + \frac{\dot{x}_{2p}}{\sqrt{1+D^2}})e^{-\sqrt{1+D^2}\tau_p}$.

The same happens with the unstable solutions for $\hat{\lambda} \geqslant 1$, as we can see from Eq. (31) for $\tau \to \infty$. Two examples of the last kind of unstable solution, corresponding to the full circles in Fig. 2 are shown in curves (c) and (d) of Fig. 5 for $\hat{\xi} = 0.3$ and $\hat{\lambda} = 1.1$ and 1.5, respectively.

Eventually, for cases placed far enough from the stability region ($\hat{\xi} \gg \hat{\xi}_{\rm th}$, $\hat{\lambda} \gg 1$) all the unstable solutions have a growth rate that approaches the classical value $\sqrt{A_T kg}\sigma_\infty$ [Fig. 5, curve (e)]. A similar behavior was

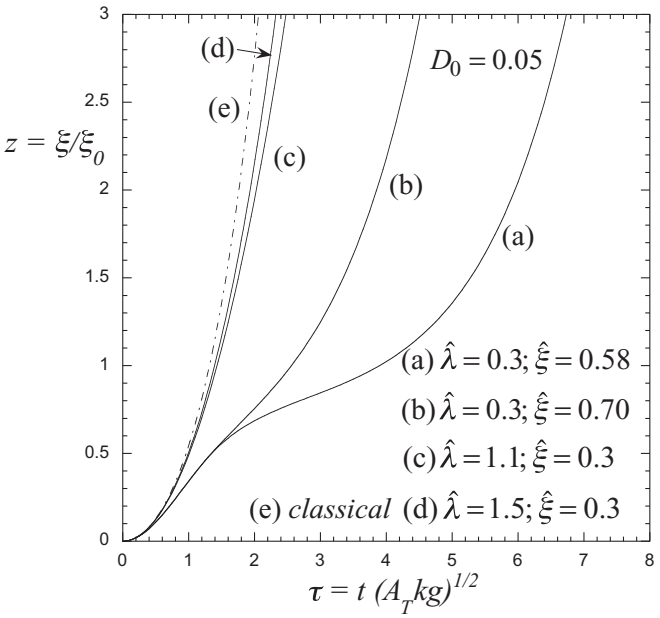

FIG. 5. Unstable solutions. (a) and (b) $\hat{\lambda} \leqslant 1$ and $\hat{\xi} \geqslant \hat{\xi}_{\rm th}$. (c) and (d) $\hat{\lambda} \geqslant 1$. (e) Classical viscous case.

observed for elastoplastic-solid–inviscid-fluid interfaces in Refs. [46,47].

It is important to notice that both stable and unstable cases present particular features that depend only on the viscosity of the liquid phase, independently of the mechanical properties of the elastoplastic solid. Thus, they could be used as a tool for measuring the viscosity of melted metals under extreme conditions relevant to geophysics and planetary sciences [49–52]. In fact, the elastic oscillations of the stable solutions taking place after the maximum amplitude z_m are damped as $e^{-D\tau}$ so that this damping is determined only by the liquid viscosity. In the same manner, the asymptotic linear growth rate of all the unstable solutions given by Eq. (33) does not depend on the solid's mechanical properties. Thus, provided that the linear growth regime is accessible to experimental measurements, the RTI could be used for determining the viscosity of melted metals in a manner similar to the way it is currently used for evaluating the yield strength of solids.

III. CONCLUDING REMARKS

We have used a previous model for the linear growth of the RTI at an interface between an elastoplastic solid and a viscous liquid to calculate the time evolution of the perturbation amplitude in different regions of the space parameters $(\hat{\xi},\hat{\lambda})$ and to evaluate the effect of the liquid viscosity on them. The understanding of the behavior of the RTI at such types of interface is required for analysis of the performance of the LAPLAS experiment at the FAIR facility. In addition, LAPLAS has recently been included in the research program that will be undertaken in the new Heavy Ion Facility (HIAF) under planning at the Institute of Modern Physics of the Chinese Academy of Sciences.

We find that both stable and unstable solutions present features that depend exclusively on the liquid viscosity, apart from the externally imposed experimental conditions. Therefore, they can be used as a tool for the experimental determination of the viscosity of liquid metals under conditions that are of great relevance to geophysics and planetary sciences, in a similar manner to the way the RTI is currently used for evaluating solid mechanical properties. Namely, the stable time evolutions of the perturbation performs purely elastic oscillations after achieving its maximum amplitude, and these oscillations are damped only because of the liquid viscosity. Certainly, the linear regime that we have studied here may not be easily accessible to experimental measurements. However, in Ref. [22] experiments on the RTI in solids are reported in which sinusoidal corrugations with $\xi_0 = 0.6$ μm and $\lambda = 60$ and 100 μm were machined on a vanadium plate, so that $k\xi_0 \leqslant 0.06$. Therefore, the conditions for the realization of RTI experiments in the linear regime for measuring the viscosity as proposed in this work may not be beyond present experimental possibilities.

On the other hand, we can see that all the unstable time evolutions grow with an asymptotic growth rate corresponding to an interface between an ideal fluid and a viscous liquid given by Eq. (33). A similar behavior was observed in Refs. [46,47] for the RTI at the interface between an elastic solid and ideal fluid for which the asymptotic growth rate was equal to $\sqrt{kg}$, as in the classical case. This feature could indicate that the mechanical properties of the solid will not affect the late RTI evolution in the nonlinear regime, except for the memory saved in the "effective" initial amplitude in Eq. (33).

ACKNOWLEDGMENTS

This work has been partially supported by the Ministerio de Economía y Competitividad of Spain (Grant No. ENE2009-09276), by the BMBF of Germany, and by the Chinese Academy of Sciences.

[1] J. W. Miles, General Dynamics Report No GAMD-7335, AD 643161, 1966 (unpublished).
[2] G. N. White, Los Alamos National Laboratory Report No LA-5225-MS, 1973 (unpublished).
[3] J. F. Barnes, P. J. Blewet, R. G. McQueen, K. A. Meyer, and D. Venable, J. Appl. Phys. **45**, 727 (1974).
[4] J. F. Barnes, D. H. Janney, R. K. London, K. A. Meyer, and D. H. Sharp, J. Appl. Phys. **51**, 4678 (1980).
[5] J. K. Dienes, Phys. Fluids **21**, 736 (1978).
[6] J. W. Swegle and A. C. Robinson, J. Appl. Phys. **66**, 2838 (1989).
[7] A. C. Robinson and J. W. Swegle, J. Appl. Phys. **66**, 2859 (1989).
[8] D. C. Drucker, in *Mechanics Today*, edited by S. Nemmat-Nasser (Pergamon, Oxford, 1980), Vol. 5, p. 37.
[9] D. C. Drucker, Ing. Arch. **49**, 361 (1980).
[10] E. L. Ruden and D. E. Bell, J. Appl. Phys. **82**, 163 (1997).
[11] G. Dimonte, R. Gore, and M. Schneider, Phys. Rev. Lett. **80**, 1212 (1998).
[12] G. Dimonte, Phys. Plasmas **6**, 2009 (1999).
[13] P. N. Nizovtzev and P. N. Raevskii, Kvantovaya Electron. (Kiev) **3**, 11 (1991).

[14] A. I. Lebedev, P. N. Nizovtzev, P. N. Raevskii, and V. P. Solovev, Phys. Dokl. **41**, 328 (1996).
[15] S. M. Bakharakh, O. B. Drennov, N. P. Kovalev, A. I. Lebedev, E. E. Meshkov, A. L. Mikhailov, N. V. Neumerzhitsky, P. N. Nizovtsev, V. A. Rayevsky, G. P. Simonov, V. P. Solovyev, and I. G. Zhidov, Lawrence Livermore National Laboratory Report No. UCRL-CR-126710, 1997 (unpublished).
[16] D. H. Kalantar, B. A. Remington, J. D. Colvin, K. O. Mikaelian, S. V. Weber, L. G. Wiley, J. S. Wark, A. Loveridge, A. M. Allen, A. A. Hauer, and M. A. Meyers, Phys. Plasmas **7**, 1999 (2000).
[17] J. D. Colvin, M. Legrand, B. A. Remington, G. Shurtz, and S. V. Weber, J. Appl. Phys. **93**, 5287 (2003).
[18] B. A. Remington, P. Allen, E. M. Bringa, J. Hawreliak, D. Ho, K. T. Lorenz, H. Lorenzana, J. M. McNaney, M. A. Meyers, S. W. Pollaine, K. Rosolankova, B. Sadik, M. S. Schneider, D. Swift, J. Wark, and B. Yaakobi, Mater. Sci. Technol. **22**, 474 (2006).
[19] A. R. Piriz, J. J. López Cela, N. A. Tahir, and D. H. H. Hoffmann, Phys. Rev. E **74**, 037301 (2006).
[20] G. Dimonte, G. Terrones, F. J. Cherne, T. C. Germann, V. Dupont, K. Kadau, W. T. Buttler, D. M. Oro, C. Morris, and D. L. Preston, Phys. Rev. Lett. **107**, 264502 (2011).
[21] K. O. Mikaelian, Phys. Plasmas **17**, 092701 (2010).
[22] H-S. Park, K. T. Lorenz, R. M. Cavallo, S. M. Pollaine, S. T. Prisbrey, R. E. Rudd, R. C. Becker, J. V. Bernier, and B. A. Remington, Phys. Rev. Lett. **104**, 135504 (2010).
[23] G. H. Houseman and P. Molnar, Geophys. J. Int. **128**, 125 (1997).
[24] E. B. Burov and P. Molnar, Earth Planet. Sci. Lett. **275**, 370 (2008).
[25] W. Gorczyk, B. Hobbs, K. Gessner, and T. Gerya, Gondwana Res. **24**, 838 (2013).
[26] W. Gorczyk and K. Vogt, Gondwana Res. (to be published).
[27] O. Blaes, R. Blandford, and P. Madau, Astrophys. J. **363**, 612 (1990).
[28] N. A. Tahir, D. H. H. Hoffmann, A. Kozyreva, A. Tauschwitz, A. Shutov, J. A. Maruhn, P. Spiller, U. Neuner, J. Jacoby, M. Roth, R. Bock, H. Juranek, and R. Redmer, Phys. Rev. E **63**, 016402 (2000).
[29] A. R. Piriz, R. F. Portugues, N. A. Tahir, and D. H. H. Hoffmann, Phys. Rev. E **66**, 056403 (2002).
[30] N. A. Tahir, H. Juranek, A. Shutov, R. Redmer, A. R. Piriz, M. Temporal, D. Varentsov, S. Udrea, D. H. H. Hoffmann, C. Deutsch, I. Lomonosov, and V. E. Fortov, Phys. Rev. B **67**, 184101 (2003).
[31] N. A. Tahir, A. Shutov, D. Varentsov, P. Spiller, S. Udrea, D. H. H. Hoffmann, I. Lomonosov, J. Wieser, M. Kirk, A. R. Piriz, V. E. Fortov, and R. Bock, Phys. Rev. Spec. Top.–Accel. Beams **6**, 020101 (2003).
[32] M. Temporal, A. R. Piriz, N. Grandjouan, N. A. Tahir, and D. H. H. Hoffmann, Laser Part. Beams **21**, 609 (2003).
[33] N. A. Tahir, C. Deutsch, V. E. Fortov, V. Gryaznov, D. H. H. Hoffmann, M. Kulish, I. V. Lomonosov, V. Mintsev, P. Ni, D. Nikolaev, A. R. Piriz, N. Shilkin, P. Spiller, A. Shutov, M. Temporal, V. Ternovoi, S. Udrea, and D. Varentsov, Phys. Rev. Lett. **95**, 035001 (2005).
[34] N. A. Tahir, P. Spiller, S. Udrea, O. D. Cortazar, C. Deutsch, V. E. Fortov, V. Gryaznov, D. H. H. Hoffmann, I. V. Lomonosov, P. Ni, A. R. Piriz, A. Shutov, M. Temporal, and D. Varentsov, Nucl. Instrum. Methods Phys. Res. Sect. B **245**, 85 (2006).
[35] N. A. Tahir, A. Shutov, I. V. Lomonosov, A. R. Piriz, G. Wouchuk, C. Deutsch, D. H. H. Hoffmann, and V. E. Fortov, High Energy Density Phys. **2**, 21 (2006).
[36] N. A. Tahir, Th. Stoehlker, A. Shutov, I. V. Lomonosov, V. E. Fortov, M. French, N. Nettelmann, R. Redmer, A. R. Piriz, C. Deutsch, Y. Zhao, P. Zhang, H. Xu, G. Xiao, and W. Zhan, New J. Phys. **12**, 073022 (2010).
[37] R. E. Reinovsky, W. E. Anderson, W. L. Atchison, C. E. Ekdahl, R. J. Faehl, I. R. Lindemuth, D. V. Morgan, M. Murillo, J. L. Stokes, and J. S. Shlachter, IEEE Trans. Plasma Sci. **30**, 1764 (2002).
[38] R. D. McBride *et al.*, Phys. Plasmas **20**, 056309 (2013).
[39] B. J. Plohr and D. H. Sharp, Z. Angew. Math. Phys. **49**, 786 (1998).
[40] G. Dimonte, P. Ramaprabhu, and M. Andrews, Phys. Rev. E **76**, 046313 (2007).
[41] A. R. Piriz, J. J. López Cela, and N. A. Tahir, Phys. Rev. Lett. **105**, 179601 (2010).
[42] G. Terrones, Phys. Rev. E **71**, 036306 (2005).
[43] A. R. Piriz, J. J. López Cela, O. D. Cortázar, N. A. Tahir, and D. H. H. Hoffmann, Phys. Rev. E **72**, 056313 (2005).
[44] A. R. Piriz, O. D. Cortazar, J. J. López Cela, and N. A. Tahir, Am. J. Phys. **74**, 1095 (2006).
[45] J. J. LópezCela, A. R. Piriz, M. C. Serna Moreno, and N. A. Tahir, Laser Part. Beams **24**, 427 (2006).
[46] A. R. Piriz, J. J. López Cela, and N. A. Tahir, J. Appl. Phys. **105**, 116101 (2009).
[47] A. R. Piriz, J. J. López Cela, and N. A. Tahir, Phys. Rev. E **80**, 046305 (2009).
[48] A. R. Piriz, Y. B. Sun, and N. A. Tahir, Phys. Rev. E **88**, 023026 (2013).
[49] G. H. Millerand and T. J. Ahrens, Rev. Mod. Phys. **63**, 919 (1991).
[50] V. N. Mineev and A. I. Funtikov, Phys. Usp. **47**, 671 (2004).
[51] Y. L. Li, F. S. Liu, X. J. Ma, Y. G. Li, M. Yu, J. C. Zhang, and F. Q. Jing, Rev. Sci. Instrum. **80**, 013903 (2009).
[52] K. O. Mikaelian, Phys. Rev. E **87**, 031003 (2013).
[53] A. S. Khan and S. Huang, *Continuous Theory of Plasticity* (J. Wiley and Sons, New York, 1995).
[54] A. R. Piriz, J. J. López Cela, N. A. Tahir, and D. H. H. Hoffmann, Phys. Rev. E **78**, 056401 (2008).
[55] A. R. Piriz, N. A. Tahir, D. H. H. Hoffmann, and M. Temporal, Phys. Rev. E **67**, 017501 (2003).
[56] A. R. Piriz, M. Temporal, J. J. LópezCela, N. A. Tahir, and D. H. H. Hoffmann, Plasma Phys. Controlled Fusion **45**, 1733 (2003).
[57] A. Bret, A. R. Piriz, and N. A. Tahir, Phys. Rev. E **85**, 036402 (2012).